Supplementary Information

Nanoamplifiers Synthesized from Gadolinium and Gold Nanocomposites for Magnetic Resonance Imaging

Xiumei Tian [a,b], Yuanzhi Shao [c], Haoqiang He [a], Huan Liu [c], Yingying Shen [a], Wenlin Huang [*a,d] and Li Li [*a]

[a]State Key Laboratory of Oncology in South China, Sun Yat-sen University Cancer Center, Guangzhou 510060, People's Republic of China

[b]Department of Biomedical Engineering, Guangzhou Medical College, Guangzhou 510182, People's Republic of China

[c]State Key Laboratory of Optoelectronic Materials and Technologies, School of Physics and Engineering, Sun Yat-Sen University, Guangzhou 510275, People's Republic of China

[d]CAS Key Laboratory of Pathogenic Microbiology and Immunology, Institute of Microbiology, Chinese Academy of Science, Beijing, 100054, People's Republic of China

Xiumei Tian, Yuanzhi Shao and Haoqiang He contributed equally to this work.

***Corresponding author:** li2@mail.sysu.edu.cn or wl_huang@hotmail.com

1. Characterization of Nanoamplifier

Laser Raman spectroscopy

Each sample was placed on a glass slide and measured by laser Raman spectrometer (inVia Reflex; Renishaw, Gloucestershire, UK) using excitation wavelength of 785 nm, 10 s exposure time, and 100 s integration time.

Phase-sensitive T_1 inversion recovery (PS-T1IR) imaging

Dual-modal nanoprobes and Gd_2O_3@MCM-41 silica nanocomposites were dispersed in

deionized water to various concentrations, including 0.5, 0.25, 0.1, 0.08, 0.05, 0.025, 0.0125, and 0 mM. All samples were placed into a 96 well plate and then imaged using a 3.0 T Siemens Trio MRI scanner (Siemens Medical Solutions, Erlangen, Germany) with inversion recovery at 400, 500, 600, 700, 800, 1000, 1200, and 1400 ms and repetition time (TR) of 2000 ms. Gray-scale values of the MR images were provided by PACS (Picture Archiving and Communication System) software. The data were calculated by the following formula:

$S_{IR}(T1,TE,TR)=\rho(1-2e^{-TI/T1}+2e^{-(TR-TE/2)/T1}-e^{-TR/T1})e^{-TE/T2}$

Table S1. Elemental analysis of the dual-modal nanoprobes by EDS.

Element	Weight percentage (%)	Atomic percentage (%)
O K	17.19	45.62
Si K	27.06	40.90
Cl K	1.14	1.37
Gd L	6.14	1.66
Au M	48.46	10.45
Total	100.00	

3. Immunotoxicity assays of Nanoamplifier

NO of serum assay

Peripheral blood (1 mL) were collected into Eppendorf tubes by vena ophthalmica. Place at 4℃ for 2 h, samples were subsequently centrifuged at 1000 g for 5 min at room temperature, then collected the upper serum into the tube. Add samples (50 μL) in 96-well plates, procedure according to the Griess Reagent System (Promega Corp.). The absorbance at 540 nm was measured by a microplate reader (Bio-Rad, USA).

Expression of CD80/CD86 in neutrophil

Expression of CD80/CD86was measured by flow cytometry. Peripheral blood (20 μL) was collected into a tube supplemented with heparin sodium (4 μL) by vena ophthalmica. Anti-mouse CD86-PE and anti-mouse CD80-PE were then added to the samples and incubated in dark for 30 min. Erythrocytes were lysed (2 mL) in dark for 2 min, followed by the addition of 2 mL PBS. Samples were subsequently centrifuged at 1200 g for 5 min at room temperature, followed by the addition of 400 μL PBS.

Expression of CD69 in lymphocyte cells

Expression of CD69 was measured by flow cytometry. Peripheral blood (20 μL) was

collected into a tube supplemented with heparin sodium (4 μL) by vena ophthalmica. Anti-mouse CD69-FITC were then added to the samples and incubated in dark for 30 min. Erythrocytes were lysed (2 mL) in dark for 2 min, followed by the addition of 2 mL PBS. Samples were subsequently centrifuged at 1200 g for 5 min at room temperature, followed by the addition of 400 μL PBS.

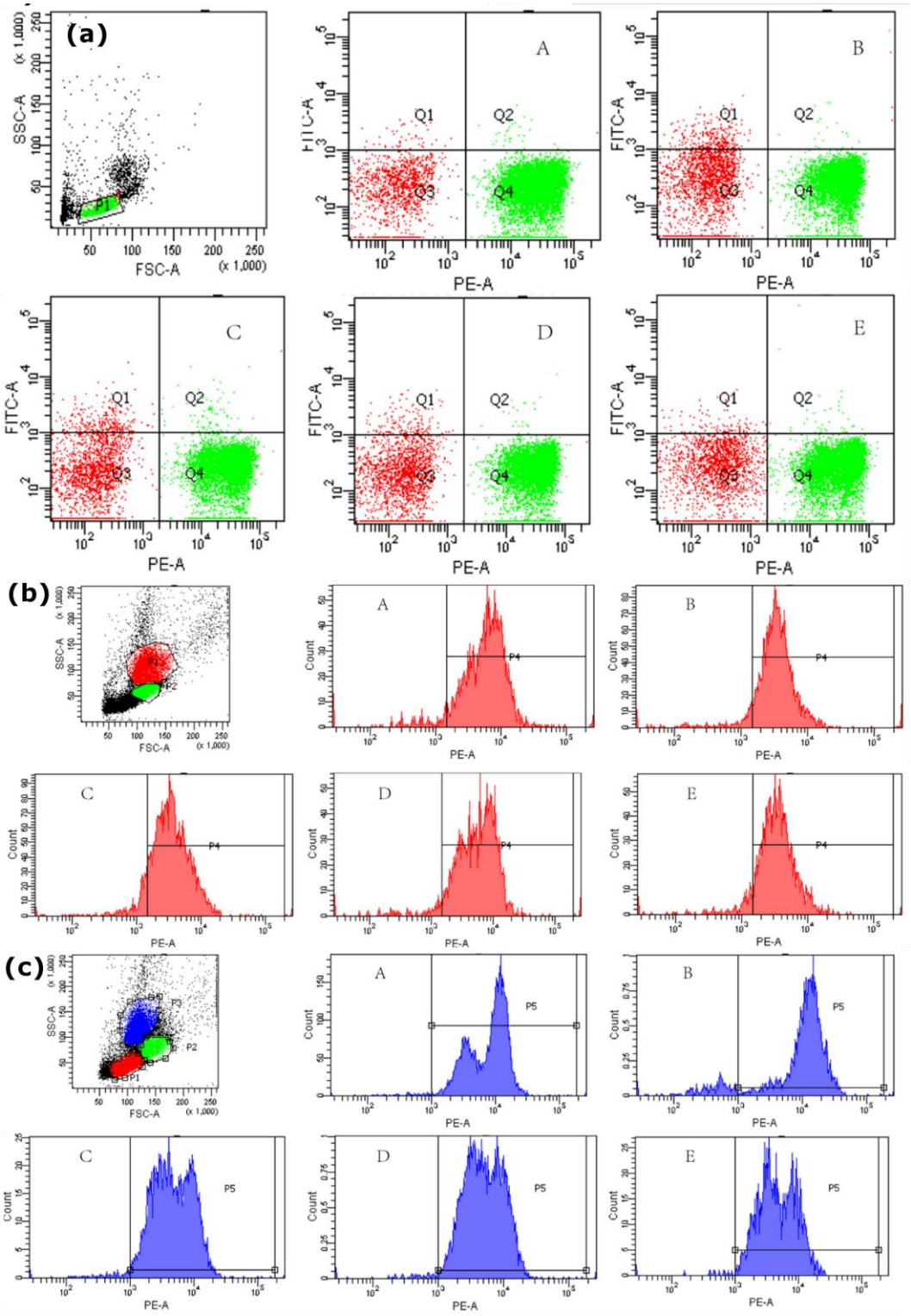

Figure S1. (a)-(c) Histogram plot of flow cytometry including CD69 expression in lymphocyte cells, CD80 and CD86 in neutrophil, respectively.

4. Half-life of Nanoamplifier in blood circulation

The half-life of the dual-modal nanoprobes in the circulation was determined by ICP-MS (n = 3 for each point) in 36 clean Kunming white mice (50% females and 50% males). Blood (5-10 μL) was drawn from the tail veins at 15, 30, 45, 60, 75, 120, 180, 240, 360, 480, 600, and 720 min after tail vein administration of the dual-modal nanoprobes (16 μmol/kg). Immediately after each blood draw, the samples were mixed with heparin sodium (85 μL) in separate eppendorf tubes. The calibration curve (Supporting Information Fig S2) was plotted at the same time.

Animal Model

All animal procedures were performed in accordance with the National Institutes of Health guidelines on the use of animals in research. Four to six-week-old Balb/c nude mice (with body weight of 19 to 23 g) were purchased from the animal experiment center of the Medical College, Sun Yat-sen University, China, and maintained in a specific pathogen-free (SPF) environment (Certificate No. 27-99S193). Mouse models of colon cancer liver metastasis were established with stable lines as follows. Human colorectal carcinoma SW480 cells were grown in PRMI-1640 media (Invitrogen, Carlsbad, CA) with 10% fetal bovine serum (FBS, Invitrogen), penicillin, streptomycin, and Geneticin (G418; 400 μg/mL; Invitrogen) at 37℃ and 5% CO_2. The colon cancer liver metastasis mouse model was established by spleen injection of the cultured SW480 cells [1×10^6 in 100 μL phosphate buffered saline (PBS)]. After 25 days of tumor cell inoculation, mice were randomized by tumor size (approximately 50 mm^3).

Optical assays

Our nanoamplifier achieved efficient optical imaging in both SW480 cells and liver tissues. Furthermore, the optical efficiency of AuNPs was not affected by PEI-degradation (Fig S4, S5).

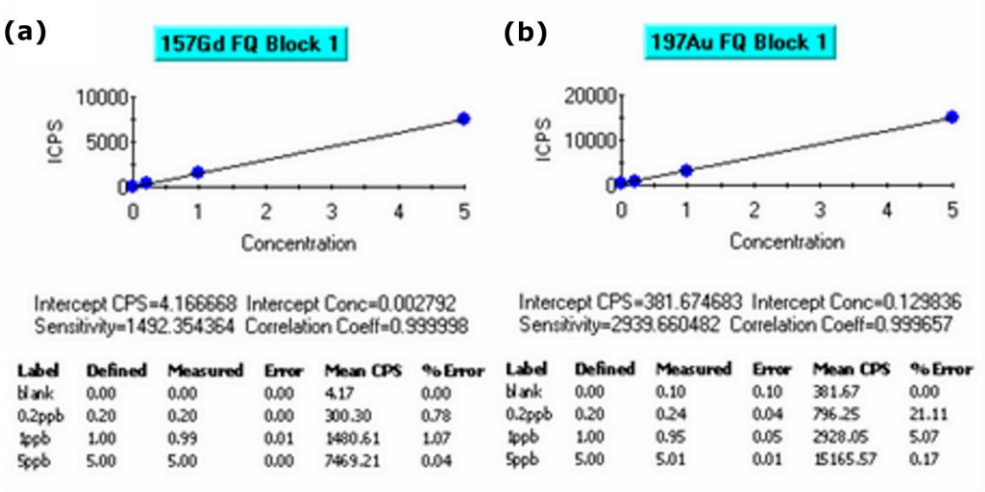

Label	Defined	Measured	Error	Mean CPS	% Error
blank	0.00	0.00	0.00	4.17	0.00
0.2ppb	0.20	0.20	0.00	300.30	0.78
1ppb	1.00	0.99	0.01	1480.61	1.07
5ppb	5.00	5.00	0.00	7469.21	0.04

Label	Defined	Measured	Error	Mean CPS	% Error
blank	0.00	0.10	0.10	381.67	0.00
0.2ppb	0.20	0.24	0.04	796.25	21.11
1ppb	1.00	0.95	0.05	2928.05	5.07
5ppb	5.00	5.01	0.01	15165.57	0.17

Figure S2: Comparison between the serum Gd/Au ratios and the control (Gd/Au ratio in uninjected nanoprobes) at different time points.

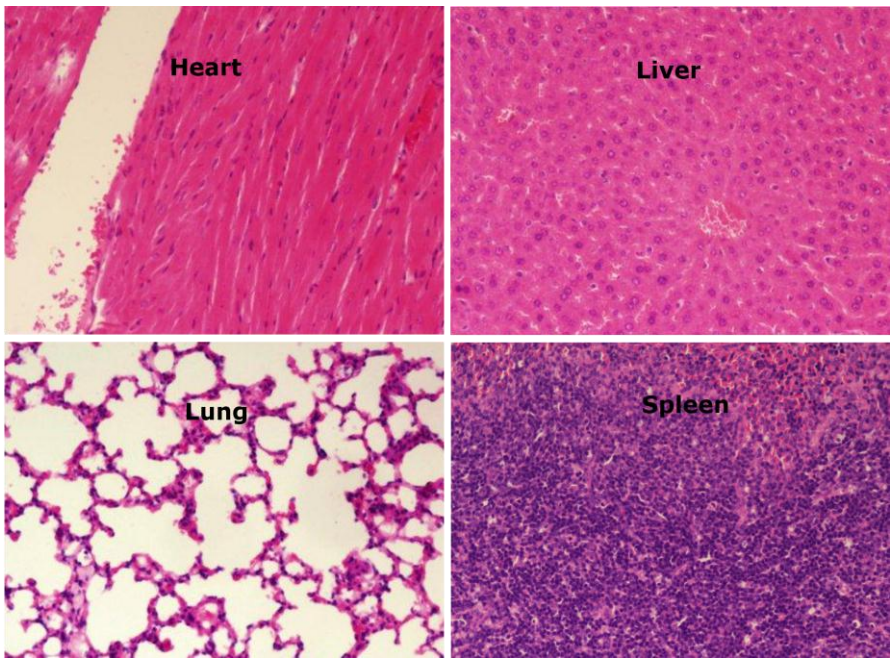

Figure S3: Tissues were collected 4 h after injection of the dual-modal nanoprobes (16 μmol/kg), stained with hematoxylin and eosin, and imaged under a light microscope at 200 × magnification.

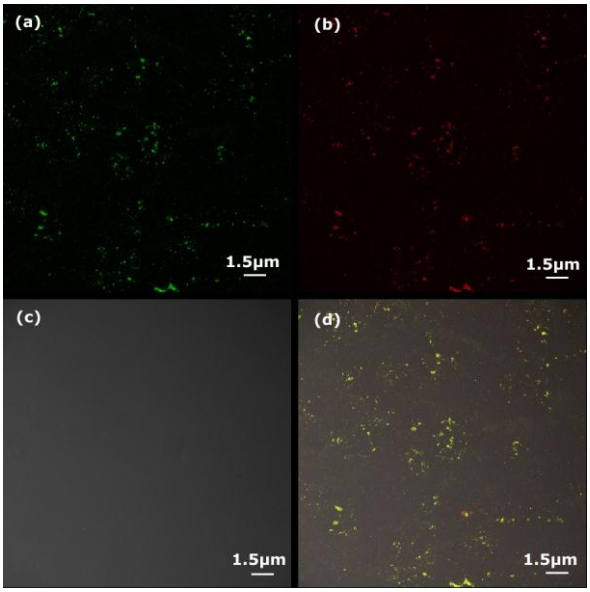

Figure S4. Optical images of liver without HE were obtained by confocal microscopy in mice 4 h after intravenous administration of nanoamplifier (8 μmol/kg). (a) (b) Fluorescence imaging at 525nm of excitation wavelength, (c) Bright field imaging, (d) the imaging is merged with (a), (b) and (c) imaging.

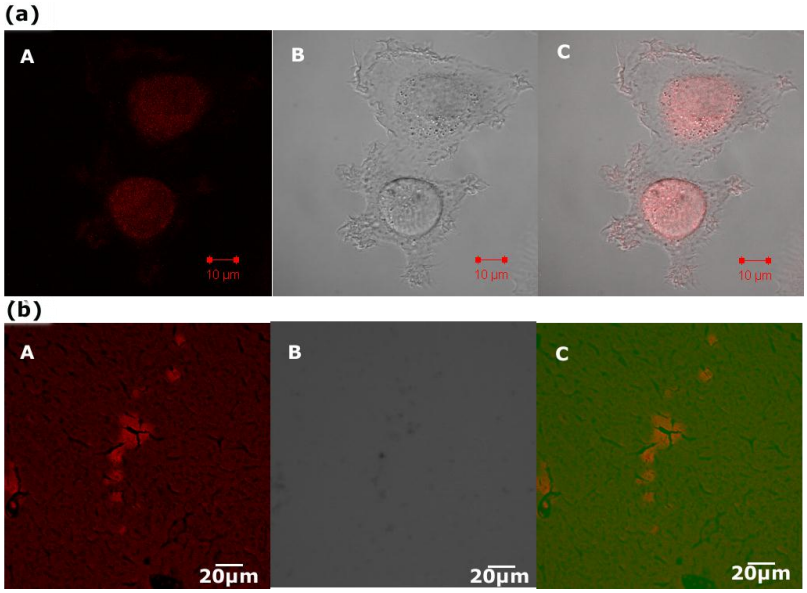

Figure S5. Optical images of nanoamplifier were obtained by confocal microscopy. (a) SW480 colon cancer cells incubated in media with 100 μmol/L nanoamplifier for 12 h. (b) The liver of mice was measured at 4 h after intravenous administration of nanoamplifier (8 μmol/kg). (A) Fluorescence imaging at 525nm of excitation wavelength, (B) Bright field imaging, (C) the A imaging is merged with the B imaging

Table S2. Concentration of Gd (ng/g) measured by ICP-MS in various organs of our mice model (n = 3) at specific times after intravenous injection of the nanoprobes (16 μmol/kg).

Gd (ng/g, mean±S.E)	4 h	10 h	24 h	3 months

Brain	1059.71±94.07	732.52±37.54	477.21±20.54	227.79±13.44
Liver	5929.86±119.44	17036.81±456.01	45938.02±671.39	12279.4±98.07
Lung	333437.5±287.48	266594.8±677.04	110364.1±1008.53	64998.23±1323.83
Spleen	111076.9±6555.87	117236.3±575.87	119653.5±1206.8	53920.68±1047.61
Heart	1854.61±65.11	1608.9±87.43	1251.58±36.4	3289.71±39.08
Kidney	2097.22±30.75	2410.46±56.9	2926.56±21.37	1003.72±18.35
Cancer	275±15.2	3165.91±55.26	4384.38±43.89	—

Table S3. Concentration of Au (ng/g) measured by ICP-MS in various organs of our mice model (n = 3) at specific times after intravenous injection of the nanoprobes (16 μmol/kg).

Au (ng/g, mean±S.E)	4 h	10 h	24 h	3 months
Brain	2645.88±87.46	1703.63±28.05	656.62±21.45	66.62±3.14
Liver	5542.99±107.54	37180.66±1329.51	51591.29±679.31	20013.52±398.6
Lung	40000±3058.65	29941.07±559.39	10288.83±1080.72	3652.65±132.38
Spleen	101096.2±8545.06	100594.2±2186.46	96806.93±1208.6	49334.483±1174.66
Heart	1324.67±65.02	1803.71±60.04	2077.22±34.36	360.66±29.8
Kidney	842.26±30.57	1196.25±46.22	1536.72±20.73	682.31±19.5
Cancer	768.75±15.92	4334.1±85.7	6618.75±134.98	—